Special Issue: Recent advances (2008 – 2015) in the study of ground ice and cryostratigraphy

Article (Accepted Version)

Recent Advances (2008 – 2015) in the Study of Ground Ice and Cryostratigraphy

Graham L. Gilbert[1 2*], Mikhail Kanevskiy[3], Julian B. Murton[4]

[1] Department of Arctic Geology, The University Centre in Svalbard, Longyearbyen, Norway

[2] Department of Earth Science, The University of Bergen, Bergen, Norway

[3] Institute of Northern Engineering, University of Alaska Fairbanks, Fairbanks, AK, USA

[4] Permafrost Laboratory, Department of Geography, University of Sussex, Brighton, UK

*** Correspondence to:**

Graham L. Gilbert

Arctic Geology Department, The University Centre in Svalbard, UNIS, P.O: Box 156, 9171 Longyearbyen, Norway.

E-mail: graham.gilbert@unis.no

Keywords: Cryostratigraphy; Ground Ice; Permafrost; Cryostructures

ABSTRACT

Cryostratigraphy involves the description, interpretation and correlation of ground-ice structures (cryostructures) and their relationship to the host deposits. Recent advances in the study of ground ice and cryostratigraphy concern permafrost aggradation and degradation, massive-ice formation and evaluation of ground-ice content. Field studies have increased our knowledge of cryostructures and massive ground ice in epigenetic and syngenetic permafrost. Epigenetic permafrost deposits are relatively ice-poor and composed primarily of pore-filled cryostructures, apart from an ice-enriched upper section and intermediate layer. Syngenetic permafrost deposits are commonly identified from cryostructures indicative of an aggrading permafrost table and are characterized by a high ice content, ice-rich cryofacies, and nested wedge ice. Degradation of ice-rich permafrost can be marked by thaw unconformities, truncated buried ice wedges, ice-wedge pseudomorphs, and organic-rich 'forest beds'. Studies of massive ground ice have focused on wedge ice, thermokarst-cave ice, intrusive ice, and buried ice. Significant advances have been made in methods for differentiating between tabular massive ice bodies of glacier and intrasedimental origin. Recent studies have utilized palynology, isotope geochemistry and hydrochemistry, in addition to sedimentary and cryostratigraphic analyses. The application of remote sensing techniques and laboratory methods such as CT scanning has improved estimations of the ice content of frozen sediments.

INTRODUCTION

Cryostratigraphy concerns the distribution and organization of ground ice in soil, sediment, or bedrock. It can be defined as "the study of layering within permafrost; based on the description and interpretation of ice, sediment and rock, cryostratigraphy identifies and correlates stratigraphic units – usually layers – of permafrost" (Murton, 2013, p. 174). The value of cryostratigraphy stems from the fact that ground ice within sediment produces structures whose identification can elucidate the thermal history and origin of the substrate, because ground-ice formation, morphology, and preservation are influenced by various climatic, geologic, and environmental factors (Katasonov, 2009; French and Shur, 2010; Popov, 2013; Murton, 2013). Ground ice may be preserved indefinitely in permafrost environments, providing an enduring palaeoenvironmental archive. The principles of cryostratigraphy and general problems related to ground ice studies have been recently discussed in English (French and Shur, 2010; Y. K. Vasil'chuk, 2012; Murton, 2013) and in Russian (Rogov, 2009; Badu, 2010; Shpolyanskaya, 2015).

Ice-rich permafrost is commonly associated with frost-susceptible sediment and occurs where moisture is sufficient for ground-ice formation or where ice is buried (Murton, 2013). Conditions conducive to extensive ground-ice formation have existed for much of the Quaternary Period in Arctic and Subarctic lowlands underlain by fine-grained sediments. Hence, the geographical distribution of recent cryostratigraphic studies has focused mainly on northern and central Siberia, Alaska and western Arctic Canada (Figure 1).

This review identifies recent advances in the understanding of ground ice and cryostratigraphy of present-day permafrost regions based on literature published between 2008 and 2015. We focus on four cryostratigraphic themes: (1) permafrost aggradation, (2) renewed aggradation of permafrost following degradation, (3) massive ground ice, and (4)

evaluation of ground-ice content. The dating of permafrost and the cryostratigraphy of past permafrost regions (e.g. northwest Europe) are beyond the scope of this review.

PERMAFROST AGGRADATION

Cryostratigraphic reconstructions of permafrost aggradation tend to focus on ground-ice development in unconsolidated sediments and classify permafrost in terms of its time of formation relative to the deposition of the host material. *Epigenetic permafrost* aggrades after the host material has formed, sometimes with a time lag of thousands or millions of years (French and Shur, 2010). *Syngenetic permafrost* aggrades at a rate proportional to the sedimentation rate at the ground surface, and characterizes cold-climate landscapes influenced by relatively continuous deposition by fluvial, colluvial, lacustrine, or aeolian processes. *Quasi-syngenetic permafrost* forms the top layer of permafrost (ice-rich intermediate layer) by upwards freezing as a result of the gradual thinning of the active layer over time – usually due to the development of surface vegetation (Shur, 1988). Many permafrost bodies consist of epigenetic, syngenetic, and/or quasi-syngenetic components and so are *polygenetic*. The distinction between them is made by systematically analyzing the spatial distribution of cryostructures and the nature of ground ice.

Cryostructures, or patterns formed by ice inclusions in frozen ground, are defined as structures that reflect the amount and distribution of pore and segregated ice within frozen sediment (French and Shur, 2010). Individual cryostructures are identified based on the shape, distribution and proportions of ice, sediment or rock within frozen ground (Murton, 2013). Nine cryostructures are commonly described in recent literature (Figure 2A-I). (A) *Pore* cryostructure develops where pore water freezes *in situ* in the interstices between mineral grains, forming an ice cement; the pore cryostructure may be visible to the naked eye in sands and gravels or nonvisible in silts or clays. (B) *Organic-matrix* cryostructure forms

where ice fills void spaces in organic material (e.g. peat or organic-rich soil). (C) *Crustal* cryostructure occurs where ice segregation creates an ice crust around an object such as a rock clast or wood fragment in frost-susceptible material. (D) *Vein* cryostructure denotes ice veins that are inclined to vertical in orientation. (E) *Lenticular* cryostructure denotes lens-shaped ice bodies, often horizontal to subhorizontal, formed by ice segregation in frost-susceptible material. (F) *Layered* (or bedded) cryostructure comprises horizontal to dipping ice layers formed by ice segregation or injection of pressurized water. (G) *Reticulate* cryostructure represents a three-dimensional network of vertical ice veins and horizontal ice lenses that separate clayey or silty sediment blocks. (H) *Ataxitic* (suspended) cryostructure develops where sediment grains or aggregates are suspended in ice; in many cases it forms in the intermediate layer at the top of permafrost. (I) *Solid* cryostructure occurs where bodies of ice exceed 10 cm in thickness. These cryostructures are useful for logging of permafrost sequences, but in reality some cryostructures are transitional, composite or hierarchical in nature (Murton, 2013).

The development of cryostructures relates to three main factors: (1) the physical properties of soil, sediment, or bedrock; (2) moisture availability; and (3) the mode of permafrost formation (epigenetic, syngenetic, or quasi-syngenetic). A key property is the grain-size distribution (particularly the proportion of silt) and packing of grains, which influence the frost susceptibility of the host sediment (i.e. the degree to which the soil favours the formation of segregated ice). Frost susceptibility in soils depends primarily on the continuous network of unfrozen water films in the frozen fringe. Moister sites promote the formation of ice-rich cryostructures compared to drier ones (Murton, 2013; Stephani *et al.*, 2014).

Distinguishing cryostructures is scale-dependent and may be difficult when working with cores. The small diameter of cores (mostly between 5 cm and 10 cm) means that lateral continuity of ground-ice bodies in many cases cannot be established. For instance, it may not

be possible to distinguish between lenticular and layered cryostructures at the core scale. Natural sections or trial pits best reveal cryostructures.

Epigenetic Permafrost

When the ground surface begins to experience cold subaerial conditions, epigenetic permafrost aggrades downward. Under such conditions, ground ice and permafrost decrease in age with depth.

Outside of areas with buried ice, epigenetic permafrost tends to be ice-poor, with wedge and segregated ice concentrated mostly in the top few meters. However, ice-rich epigenetic permafrost (including massive-ice bodies of segregated or intrusive origin) may form at any depth where the freezing front encounters a significant source of ground water. The distance between visible ice lenses generally increases with depth, whereas the overall ice content decreases. The ice-rich top, in many cases, may be explained by the formation of the ice-rich intermediate layer, which results from a gradual decrease in active-layer thickness (mostly due to accumulation of organic matter) and is characterized by an ataxitic (suspended) cryostructure (French and Shur, 2010). Formation of the intermediate layer is considered "quasi-syngenetic" because permafrost aggrades upward without any sedimentation on the ground surface (Shur *et al.*, 2011).

Cryostructures of ataxitic, lenticular and layered type are common in the intermediate layer (Osterkamp *et al.*, 2009; Calmels *et al.*, 2012). The type of cryostructure in this layer depends strongly on the rate of upward permafrost aggradation. Prolonged stability of the permafrost table favours layered cryostructures (so-called 'ice belts', discussed below), whereas slow aggradation of the permafrost table favours ataxitic cryostructures (Calmels *et al.*, 2012), as illustrated from till deposits in Yukon, Canada (Stephani *et al.* 2014).

Where groundwater supply is limited, epigenetic freezing forms a pore cryostructure with very low ice content (Stephani *et al.*, 2014), whose presence in frost-susceptible material is a hallmark of epigenetic permafrost. Reticulate cryostructures also indicate epigenetic permafrost, and are believed to develop by desiccation and shrinkage during sediment freezing while moisture migrates towards an advancing freezing front (French and Shur, 2010).

Ice-rich epigenetic permafrost commonly forms in sediments where groundwater is abundant. Layered and reticulate cryostructures characterize epigenetically frozen lacustrine silts in the lowlands of west-central Alaska, with the volume of visible segregated ice varying from 10 to 50%, and ice lenses up to 10 cm thick (Kanevskiy *et al.*, 2014). Similar cryostructures have been described in Nunavik, Canada (Calmels and Allard, 2008). Ice-rich epigenetic permafrost was also detected near Anchorage, close to the southern boundary of permafrost in Alaska (Riddle and Rooney, 2012). In the 10-m-thick section of glacio-lacustrine deposits (silty clay with numerous layers of segregated ice up to 70 cm thick) there, the average volume of visible ice exceeded 40% (Kanevskiy *et al.*, 2013a).

In the discontinuous permafrost zone, epigenetic permafrost often starts to form with the development of palsas or lithalsas, which may eventually transform into permafrost plateaus elevated above the initial ground surface by accumulation of segregated ice. Palsas and lithalsas have been recently studied in Fennoscandia (Seppälä, 2011); the Altai and Sayan regions of Russia (Iwahana *et al.*, 2012; Y. K. Vasil'chuk *et al.*, 2015); NWT (e.g. Wolfe *et al.*, 2014) and northern Quebec, Canada (Kuhry, 2008; Calmels and Allard, 2008; Calmels *et al.*, 2008); the Himalayas (Wünnemann *et al.*, 2008); and Mongolia (Sharkuu *et al.*, 2012).

Ice-rich syngenetic permafrost sometimes degrades, drains, and subsequently re-establishes as epigenetic permafrost. Thawed and refrozen soils typically undergo a reduction in ice content when compared with their former state. However, in many cases ice-rich, quasi-

158 syngenetic permafrost forms on top of such refrozen soils, usually due to the development of
159 surface vegetation and formation of an organic-rich surface horizon (Stephani *et al.*, 2014;
160 Kanevskiy *et al.*, 2014).
161 Bedrock hosts epigenetic permafrost in many areas, especially alpine settings and areas
162 eroded by Pleistocene glaciers, for example the Canadian Shield. Classification of
163 cryostructures in bedrock adopted from the Russian permafrost literature (translated by
164 Mel'nikov and Spesivtsev, 2000) is presented by French and Shur (2010). Pore and layered
165 cryostructures in basalt lava have recently been described from Kamchatka (Abramov *et al.*,
166 2008) and intrusive ice layers and lenses in limestones, dolomites, marls and kimberlites from
167 central Yakutia (Alexeev *et al.*, 2016).
168
169 **Syngenetic Permafrost**
170 Ground ice in syngenetic permafrost forms within aggrading sedimentary sequences during
171 or soon after deposition, mainly as segregated ice at the top of permafrost (also named
172 *aggradational ice;* Mackay 1972; Cheng 1983) or as syngenetic wedge ice. Layered and
173 lenticular cryostructures record the progressively aggrading ground surface, and are typical of
174 syngenetic permafrost (French and Shur, 2010). Russian studies of the 1950–1960s
175 (Katasonov, 2009; Popov, 2013) revealed a rhythmic structure of syngenetic permafrost,
176 formed by relatively uniform layers with a predominantly lenticular cryostructure separated
177 by '*ice belts*' (distinct icy layers several mm to several cm thick that indicate the position of
178 the permafrost table during periods when it was relatively stable). Cryostructures between ice
179 belts have been termed '*microcryostructures*' (Kanevskiy *et al.*, 2011), formed mainly by
180 thin (<1 mm) densely spaced ice lenses and include microlenticular, microbraided and
181 microataxitic types.

Moisture availability, soil texture, and sedimentation rate strongly control cryostructure distribution in syngenetic permafrost. Two cryofacies diagnostic of syngenetic permafrost have been distinguished in organic-rich silts, in Yukon, Canada (Stephani *et al.*, 2014). Microlenticular cryostructures formed in near-surface permafrost during periods of relatively rapid surface aggradation (e.g. by deposition of windblown silt). Conversely, ataxitic and reticulate cryostructures with thick ice belts formed during periods of slower siliciclastic sedimentation that favoured the accumulation of peat and resulted in active-layer thinning and formation of the intermediate layer. Buried ice-rich intermediate layers with thick ice belts and predominantly ataxitic cryostructure are typical of thick sequences of syngenetic permafrost (Stephani *et al.*, 2014; Kanevskiy *et al.*, 2011).

Syngenetic permafrost of Holocene age tends to be thinner than that of Pleistocene age. Currently, syngenetic permafrost forms in mineral soils within floodplains of Arctic rivers (Shur and Jorgenson, 1998), deltas (Morse and Burn, 2013), and areas of loess accumulation (Härtel *et al.*, 2012), and the reported thickness of modern syngenetic permafrost seldom exceeds 5 m. Cryostratigraphic studies of syngenetic permafrost, however, have focussed mainly on Pleistocene '*yedoma*' (or 'Ice Complex'), which represents relic ice-rich syngenetic permafrost with large ice wedges that formed in Siberia and North America during the Late Pleistocene (Figure 3A; Schirrmeister *et al.*, 2013; Murton *et al.*, 2015). Continued supply of fine-grained sediment favoured yedoma development over tens of thousands of years, producing syngenetic permafrost sequences often several tens of metres thick that archive Late Pleistocene environmental history. General maps of yedoma distribution in Siberia were presented by Konishchev (2009, 2011) and Kanevskiy *et al.* (2011), with the latter authors including a preliminary map of yedoma distribution in Alaska. Detailed maps of Siberian yedoma (scale 1:1,000,000) have been developed by Grosse *et al.* (2013) from Russian Quaternary geological maps. Yedoma sections have been recently

described from northern Yakutia (Schirrmeister *et al.*, 2011; Tumskoy, 2012; Strauss *et al.*, 2012; Wetterich *et al.*, 2011, 2014), central Yakutia (Spektor *et al.*, 2008), Taymyr (Streletskaya and Vasiliev, 2012), northern Alaska (Kanevskiy *et al.*, 2011), interior Alaska (Kanevskiy *et al.*, 2008; Meyer *et al.*, 2008), Seward Peninsula (Shur *et al.*, 2012; Stephani *et al.*, 2012), and Yukon (Froese *et al.*, 2009; Pumple *et al.*, 2015; Sliger *et al.*, 2015).

Ground ice is abundant and buried cryosols are present within many yedoma sequences. Ground ice observed at 14 locations along the coast of the Laptev and East Siberian seas was primarily wedge ice, "net-like reticulated" cryostructures, and ice bands (Schirrmeister *et al.*, 2011). The ice wedges were identified as syngenetic on the basis of their large size and morphology. Ice bands (belts in the Russian literature) were interpreted to reflect stable surface conditions and active-layer thicknesses, leading to ice-enrichment of the near-surface permafrost. Buried cryosols within the yedoma contained peat "nests" and terrestrial plant leaves and woody debris. Schirrmeister *et al.* (2011) attributed these deposits to formation subaerially in polygonal terrain.

PERMAFROST DEGRADATION AND RE-AGGRADATION

The degradation of ice-rich permafrost (thermokarst) may produce distinctive features in the cryostratigraphic record that indicate the depth or mode of past thermokarst activity prior to re-aggradation of permafrost. This is well illustrated in two case studies from yedoma regions, which are particularly susceptible to thermokarst. The first identified cryostratigraphic evidence for shallow degradation of permafrost in non-glaciated Yukon and Alaska during the last interglaciation: (1) buried relict ice wedges whose tops were thaw truncated at the base of a palaeo-active layer; (2) ice-wedge pseudomorphs formed by complete melting of ice wedges; (3) wood-rich organic silt deposits ('forest beds') that represent forest vegetation reworked by thaw slumping or deposition in thermokarst ponds or

depressions; and (4) lenticular and reticulate cryostructures interpreted as segregated ice at top of permafrost and the bottom of the active layer (Reyes *et al.*, 2010). This study inferred a depth of thaw on the order of metres during the last interglaciation, highlighting the resilience of ice-rich discontinuous permafrost over glacial-interglacial timescales. The second case study used cryostratigraphic observations to evaluate the permafrost response to clearance of surface vegetation in discontinuous permafrost of the Klondike region, Yukon (Calmels *et al.*, 2012). There, a thaw unconformity at a depth of about 2 m was interpreted to mark the thaw depth following deforestation during the gold rush era, beginning about 1900 AD.

MASSIVE GROUND ICE

Massive ice is a comprehensive term applied to large bodies of ground ice with ice contents exceeding 250% by weight (van Everdingen, 1998). Recent studies of massive ice have focused on four main genetic classes (wedge ice, thermokarst-cave (pool) ice, intrusive ice, and buried ice) and on the origin of tabular massive-ice bodies.

Wedge Ice

Ice wedges are the most common type of massive ice, and syngenetic wedges are particularly valuable in cryostratigraphy because both the wedge ice and surrounding sediments contain palaeoenvironmental archives. Syngenetic ice wedges grow both vertically and horizontally, resulting often in a vertically nested chevron pattern (Mackay, 1990). Syngenetic ice wedges in the outer Mackenzie Delta, Canada, have been identified from “shoulders” indicative of vertical growth stages and from the cross-sectional width of the wedges decreasing towards the top of permafrost (Figure 3B; Morse and Burn, 2013). The ice wedges developed below a slowly aggrading surface.

A conceptual model of syngenetic ice-wedge development invokes micro-, meso-, and macrocycles (Y. K. Vasil'chuk, 2013). Microcycles affect ice wedges by changes in active-layer depth and rates of deposition of thin sediment layers over time scales of several years to hundreds of years. Mesocycles of ice-wedge growth result from changes in water level, where ice wedges are located close to or under shallow water bodies. Deposits overlying wedge ice consist of alternating layers of peat (formed during exposure) and siliciclastic sediment (deposited during submergence). Ice-wedge growth is reduced or suspended during submergence. Macrocycles result from major changes in sedimentary regimes over time scales of tens of thousands to hundreds of thousands of years.

Syngenetic ice wedges account for a significant proportion of the ground-ice record in lowland permafrost environments, especially in yedoma. Recent studies of the isotopic or trapped gas composition in wedge ice have reconstructed palaeoclimate and investigated infilling processes (e.g. Meyer *et al.*, 2010; Opel *et al.*, 2011; Raffi and Stenni, 2011; Lachniet *et al.*, 2012). For example, Streletskaya *et al.* (2011) identified a trend of warming palaeoclimate since the Late Weichselian from different generations of syngenetic ice wedges near the Kara Sea. St-Jean *et al.* (2011) showed that site-specific factors influence the infilling characteristics of wedge ice: in cold dry settings, wedge ice shows evidence of snow densification, and in moister settings of freezing of liquid water.

Thermokarst-Cave Ice

Thermokarst-cave ice (or pool ice) forms by freezing of water trapped in underground cavities or channels (Murton, 2013), typically along degrading ice wedges (Figure 2I). Recent studies have described thermokarst-cave ice bodies underlain by silts with reticulate cryostructure in the CRREL Permafrost tunnel, interior Alaska (Fortier *et al.*, 2008; Kanevskiy *et al.*, 2008; Douglas *et al.*, 2011). Measurements performed along a 600-m-long

and 10-m-high exposure at Barter Island (Alaskan Beaufort Sea coast) showed that numerous thermokarst-cave ice bodies occupied almost 2% of the face of the coastal bluff (Kanevskiy *et al.*, 2013b).

Intrusive Ice

Intrusive ice forms by freezing of water injected under pressure into freezing or frozen ground (Murton, 2013). Recent cryostratigraphic studies of intrusive ice have focused on stable isotope stratigraphy and the identification and development of tabular massive ice.

Stable isotope analysis has been applied to reconstruct the freezing processes and growth history of pingos. Two different isotopic patterns, indicative of open-system and semi-closed system freezing, were observed in ice sections in an open-system (hydraulic) pingo in northwest Mongolia, indicating an oscillation between periods where the groundwater reservoir fed open-system ice-lens development and those of flow interruption, forming a closed-system environment (Yoshikawa *et al.*, 2013). Y. K. Vasil'chuk *et al.* (2014) distinguished between two periods of development in a closed-system (hydrostatic) pingo in northwest Siberia.

Massive bodies of intrusive ice may form following the drainage of palaeo-lake systems or from the repeated injection of lake water into marine sediments following shoreline regression. In glaciolacustrine deposits of central Yukon, Lauriol *et al.* (2010) identified, using stable O and H isotopes and occluded gas composition, intrusive ice bodies (10 m wide and 3–4 m thick) that aggraded following the lowering of water level in a palaeo-glacial lake. The glaciolacustrine sediments are underlain by permeable gravels and sands, which served as the water source during permafrost aggradation. The formation mechanism is therefore likely similar to growth conditions of hydrostatic pingos.

Buried Ice

Various types of ice bodies may be buried by soil or sediment. Recent literature on buried ice primarily concerns buried basal glacier ice (Murton, 2009; Fortier *et al.*, 2012; Solomatin and Belova, 2012; Solomatin, 2013; Coulombe *et al.*, 2015; Lacelle *et al.*, 2015) and buried snow (Spektor *et al.*, 2011). Investigations of cryostructures in basal ice from existing glaciers provide a basis for comparison with buried counterparts (e.g. Fortier *et al.*, 2012).

Several stratigraphic characteristics aid in identifying buried glacier ice, including: (1) a discordant upper contact; (2) inclusions of glacial sediment (Figure 3C); and (3) dynamic metamorphic structures. A discordant upper contact is identified by the truncation of internal ice structures such as folds, stratification, and structural and textural heterogeneities (Solomatin and Belova, 2012). Such thaw or erosional unconformities develop due to either glaciofluvial erosion or by the thaw front reaching the ice surface (Murton, 2013; Coulombe *et al.*, 2015). Glaciotectonic deformation structures in ice-rich diamictons and ice structures similar to those in modern basal glacier ice may also serve as genetic indicators. Murton (2009) used an event stratigraphy related to the timing of glaciotectonic deformation to help distinguish between massive ice that was buried or at least glacially deformed from that which postdated deformation and must be of intrasedimental origin. Though the stratigraphic context for massive ice may provide a good indication of the ice origin, it is not always conclusive, and interpretations may be strengthened by studies of ice crystallography, geochemistry and palynology.

Origin of Tabular Massive Ice

Most descriptions of tabular bodies of massive ice are from regions formerly occupied by Pleistocene glaciers or ice sheets. Such ice bodies commonly overlie coarse-grained (sand-rich) deposits, underlie fine-grained ones (muds) (Mackay and Dallimore, 1992) and contain

sediment as individual particles or aggregates. Three models are generally employed to explain the origin of massive ice: (1) intrasedimental ice growth as segregated and/or intrusive ice, (2) burial of glacier ice, and (3) subglacial permafrost aggradation (Murton, 2013). Investigations commonly combine traditional stratigraphy and cryostratigraphy with other methods (ice crystallography, geochemistry and analysis of gas inclusions).

Recent studies of tabular massive ice have been conducted along the western Arctic coast of Canada (Murton, 2009; Fritz *et al.*, 2011), central Yukon (Lauriol *et al.*, 2010), the Alaskan Coastal Plain (Kanevskiy *et al.*, 2013b), the Canadian Arctic Islands (Coulombe *et al.*, 2015), and northwest Siberia (Slagoda *et al.*, 2010, 2012a, b; Kritsuk, 2010; Leibman *et al.*, 2011; Solomatin and Belova, 2012; Fotiev, 2014, 2015; Y. K. Vasil'chuk *et al.*, 2009, 2011, 2012, 2014; Vasiliev *et al.*, 2015). Intrasedimental and buried ice have been distinguished on several lines of evidence. This includes the stratigraphic, sedimentological and geomorphological setting of the ice bodies; the upper and lower contacts between the ice and the surrounding sediments; internal characteristics of the ice body (e.g. bubble characteristics, suspended sediment and deformation structures; Figure 3D); and ice palynology, stable isotope geochemistry and hydrochemistry. However, in many cases the origin of tabular massive ice is disputed. For example, Y. K. Vasil'chuk (2012, p. 496) stated that "It should be particularly noted that presently not a single massive ice body identified in the plain areas of the permafrost regions of Russia can be definitely identified as buried glacier ice." In contrast, Solomatin and Belova (2012, p. 430) wrote in the same proceedings that "The materials, experimental data, and theoretical concepts collected at the present time lead to the clear conclusion that tabular massive ice represents a single and separate genetic type of ground ice: the buried remnants of glaciers that formed during deglaciation of the ancient glaciation areas."

Interpreting the origin of massive ice is often challenging because growth of segregated ice, intrusive ice and gradations between them can occur in both non-glacial and subglacial settings. Intrasedimental bodies of tabular massive ice frequently display characteristics similar to those of buried glacier ice (Coulombe *et al.*, 2015). Recently, however, some valuable contributions have come from studies of ice palynology, isotope geochemistry and hydrochemistry. Studies in western Siberia have suggested that pollen and spores occur in most massive-ice bodies, and although redeposited pre-Quaternary palynomorphs of Cenozoic, Mesozoic and Palaeozoic age are common, the pollen of aquatic plants, horsetail spores, limnetic diatoms and green algae remains indicate a non-glacial genesis of the ice (A. C. Vasil'chuk and Y. K. Vasil'chuk, 2010, 2012). Vasiliev *et al.* (2015) reported extremely high concentration of methane in tabular massive-ice bodies of the Yamal Peninsula, supporting the intrasedimental interpretation of tabular massive ice in this area.

Isotopic and hydrochemical analysis of massive ice is now commonly used to assist interpretation, with the values of and relations between $\delta^{18}O$, δD and d-excess providing insights in processes of fractionation, sublimation and ionic segregation during freezing (Lacelle *et al.*, 2011; Michel, 2011), including in Martian regolith (Lacelle *et al.*, 2008). Such analyses often supplement field observations of the cryostratigraphy (Murton, 2009), and have permitted identification of buried perennial snowbank ice (Lacelle *et al.*, 2009), intrusive ice (Lauriol *et al.*, 2010) and aufeis (icing ice) (Lacelle and Y. K. Vasil'chuk, 2013; Lacelle *et al.*, 2013), and basal regelation glacier ice (Fritz *et al.*, 2011, 2012).

A new classification of tabular massive ice, developed by Y. K. Vasil'chuk (2012), is based on three divisions. The first distinguishes between homogeneous and heterogeneous massive-ice bodies. *Homogeneous* massive-ice bodies have a similar genesis, composition and properties in all parts of a massive-ice complex. An example would be a single ice sill or body of massive segregated ice. *Heterogeneous* massive-ice bodies have a variable genesis,

composition and properties across a massive-ice complex, and consist of two or more homogeneous ice bodies. Numerous examples occur on the Yamal Peninsula and adjacent regions of western Siberia (Y. K. Vasil'chuk *et al.*, 2009, 2011, 2012, 2014). The second division distinguishes between *autochthonous* (intrasedimental) and *allochthonous* (buried) ice, and the third division classifies the massive ice according to its specific genetic process (e.g. injection, segregation, infiltration, burial). Overall, this classification provides a valuable framework for investigating massive ice, and emphasizes its genetic diversity.

GROUND-ICE CONTENT

Quantifying the amount and distribution of ground ice is necessary in order to predict permafrost landscape change in the future. Ground-ice content has become an important input to landscape and ecosystem models and in estimating organic carbon pools in permafrost (Kuhry *et al.*, 2013; Strauss *et al.*, 2013; Ulrich *et al.*, 2014). Cryostratigraphic observations provide valuable field data to help evaluate ground-ice content. Ground-ice content has recently been assessed using three distinct approaches: (1) landscape-scale estimation of wedge-ice volume (WIV) using remote sensing, (2) laboratory analysis of permafrost samples, and (3) fine-scale determination of ice volume by X-ray Computed Tomography (CT) scanning.

Y. K. Vasil'chuk (2009) reviewed different methods of WIV estimation (mainly based on ice-wedge geometry) developed by permafrost researchers since the 1960s. Several recent studies have estimated WIV in polygonal terrain using remotely sensed images (e.g. Bode *et al.*, 2008; Morse and Burn, 2013; Skurikhin *et al.*, 2013; Jorgenson *et al.*, 2015). Ulrich *et al.* (2014) presented a method for calculating WIV in yedoma and Holocene thermokarst basin deposits, utilizing three-dimensional (3D) surface models generated from satellite images to identify ice-wedge polygon morphometry. Individual wedge volume is estimated using

405 measurements obtained from field data. Some assumptions are employed when calculating
406 WIV: epigenetic ice wedges are usually assumed to have the shape of isosceles triangles or
407 trapezoids in cross-section (Kanevskiy *et al.*, 2013b; Ulrich *et al.*, 2014), and syngenetic ice
408 wedges that of a rectangular-shaped frontal cut (Strauss *et al.*, 2013). Ice-wedge size and
409 morphology are commonly determined by field studies. Parameters determined from field
410 measurements include the top and bottom width of individual wedges and the depth. Field
411 data are used to parameterize 3D subsurface models and to upscale to the landscape scale.
412 The ice content of sediments containing pore, segregated or intrusive ice can be
413 determined by laboratory analysis of permafrost samples. Gravimetric moisture content is
414 commonly expressed on a dry basis (the ratio of the mass of ice in a sample to the mass of the
415 dry sample). Phillips *et al.* (2015) compared dry- and wet-basis gravimetric moisture contents
416 and concluded that the latter has some advantages when used for ice-rich mineral soils.
417 Volumetric ice content (VIC) is the ratio of the volume of ice in a sample to the volume of
418 the whole sample. Excess ice content is equal to the volume in excess of the pore volume in
419 an unfrozen state, and estimations of excess ice content (e.g. O'Neill and Burn, 2012)
420 correspond to thaw strain measurements commonly performed during geotechnical
421 investigations (e.g. Kanevskiy *et al.*, 2012). In ice-rich soils, excess ice content is similar to
422 the volumetric content of visible ice. In ice-rich epigenetic permafrost, VIC can be estimated
423 relatively easily by analysing photographs of frozen cores and exposures (Kanevskiy *et al.*,
424 2013a, 2014). Total VIC of the upper layers of permafrost (which includes pore, segregated
425 and massive ice) has been estimated based on terrain-unit approach for the Beaufort Sea
426 coastal area of Alaska (Kanevskiy *et al.*, 2013b) and Yukon (Couture and Pollard, 2015).
427 CT scanning of frozen sediment cores provides a reasonable estimate of VIC and a non-
428 destructive method of 3D imaging and analyzing their internal structure (Calmels and Allard,
429 2008; Calmels *et al.*, 2010, 2012; Lapalme *et al.*, 2015). CT scans image features such as

stratification, sediment properties, fractures, gas inclusions, ice distribution and density variations. The method utilizes the density contrasts in the sample, allowing users to distinguish between gas, ice, organic and mineral components (Cnudde and Boone, 2013). Two limiting factors must be considered when determining VIC using image analysis of CT scans. Firstly, materials of similar densities are not easily differentiated. For example, organic-rich horizons (e.g. frozen, saturated peat) are similar in density to ice, which results in an overestimation of ice content unless the material can be correctly classified visually. Secondly, the spatial scan resolution (0.35 mm in the transverse directions and 0.5 mm in the longitudinal direction) limits the identification of pore ice in fine-grained sediment. Similarly, constituents (e.g. gas bubbles) that are smaller than the resolution size cannot be accounted for in volume calculations, which may lead to their underestimation, unless accounted for using calibration factors (Ducharme *et al.*, 2015).

CONCLUSIONS AND PERSPECTIVES FOR FUTURE RESEARCH

Recent cryostratigraphic research in modern permafrost environments has focused on fine-grained deposits of aeolian, fluvial, or lacustrine origin. As seen in Figure 1, however, relatively few cryostratigraphic studies have investigated permafrost in eastern Arctic Canada, Greenland and Scandinavia. Such landscapes include highly variable relief and depositional systems, where permafrost formation is closely tied to late Quaternary glacial and sea-level history. Evaluation of the cryostratigraphy of these environments may provide valuable insight into permafrost aggradation and ground-ice formation during the Holocene Epoch. Targeted studies in these locations may help to assess the nature of ground-ice formation in coarse-grained deposits, for example in alluvial fans and colluvium.

Cryostructural classifications have been successfully applied to describe the occurrence and variability of ground ice in permafrost sediment sequences. To complement these largely

descriptive and inferential studies, future research needs to investigate mechanistically the processes of cryostructure development. Freezing and thawing experiments under controlled field and laboratory conditions may allow hypothesis testing about cryostructure processes and boundary conditions, as well as quantification of rates of cryostructure formation.

The presence of ground ice has important consequences for landscape and infrastructure development as well as ecosystem and climate models. Recent studies into VIC have integrated a number of remotely sensed and indirect methods to assess ground-ice characteristics in permafrost. Future research needs to constrain the uncertainty in these estimations.

ACKNOWLEDGEMENTS

We would like to thank the two reviewers (D. Lacelle and one anonymous) and Editor C.R. Burn for their constructive comments on the manuscript. M. Kanevskiy acknowledges the National Science Foundation (NSF grants ARC 1023623 and ArcSEES 1233854) for financial support.

REFERENCES

Abramov A, Gruber S, Gilichinsky D. 2008. Mountain permafrost on active volcanoes: field data and statistical mapping, Klyuchevskaya volcano group, Kamchatka, Russia. *Permafrost and Periglacial Processes* **19** (3): 261-277. DOI: 10.1002/ppp.622.

Alexeev SV, Alexeeva LP, Kononov AM. 2016. Trace elements and rare earth elements in ground ice in kimberlites and sedimentary rocks of Western Yakutia. *Cold Regions Science and Technology* 123: 140-148. DOI: 10.1016/j.coldregions.2015.10.008

Badu YB. 2010. Cryolithology: textbook. Moscow, KDU, 528 pp. (in Russian)

Bode JA, Moorman BJ, Stevens CW, Solomon SM. 2008. Estimation of ice wedge volume in the Big Lake Area, Mackenzie Delta, NWT, Canada: In *Proceedings of the 9th International Conference on Permafrost, Fairbanks, U.S.A., 29 June-3 July 2008*, Kane DL, Hinkel KM (eds). Institute for Northern Engineering, University of Alaska Fairbanks; 131-136.

Calmels F, Allard M. 2008. Segregated ice structures in various heaved permafrost landforms through CT scan. *Earth Surface Processes and Landforms* **33**: 209-225. DOI: 10.1002/esp.1538.

Calmels F, Allard M, Delisle G. 2008. Development and decay of a lithalsa in Northern Quebec: A geomorphological history. *Geomorphology* **97**: 287-299. DOI: 10.1016/j.geomorph.2007.08.013.

Calmels F, Clavano WE, Froese DG. 2010. Progress on X-ray computed tomography (CT) scanning in permafrost studies. In *Proceedings Geo2010 Calgary – 63rd Canadian Geotechnical Conference & 6th Canadian Permafrost Conference, 12-16 September 2010, Calgary, Canada*; 1353-1358.

Calmels F, Froese DG, Clavano WR. 2012. Cryostratigraphic record of permafrost degradation and recovery following historic (1898-1992) surface disturbances in the

494 Klondike region, central Yukon Territory. *Canadian Journal of Earth Sciences* **49** (8):
495 938-952. DOI: 10.1139/e2012-023.
496 Coulombe S, Fortier D, Shur Y, Kanevskiy M, Lacelle D. 2015 Cryofacies and cryostructures
497 of massive ice found on Bylot Island, Nunavut. In *Proceedings GeoQuébec 2015– 68th*
498 *Canadian Geotechnical Conference & 7th Canadian Permafrost Conference, 20-23*
499 *September 2015, Quebec, Canada*.
500 Couture N, Pollard W. 2015. Ground ice determinations along the Yukon coast using a
501 morphological model. In *Proceedings GeoQuébec 2015– 68th Canadian Geotechnical*
502 *Conference & 7th Canadian Permafrost Conference, 20-23 September 2015, Quebec,*
503 *Canada*.
504 Cnudde V, Boone MN. 2013. High-resolution X-ray computed tomography in geosciences: A
505 review of the current technology and applications. *Earth-Science Reviews* **123**: 1-17. DOI:
506 10.1016/j.earscirev.2013.04.003.
507 Cheng G. 1983. The mechanism of repeated segregation for the formation of thick-layered
508 ground ice. *Cold Regions Science and Technology* **8**: 57-66. DOI: 10.1016/0165-
509 232X(83)90017-4.
510 Douglas TA, Fortier D, Shur Y, Kanevskiy M, Guo L, Cai Y, Bray M. 2011. Biogeochemical
511 and geocryological characteristics of wedge and thermokarst-cave ice in the CRREL
512 permafrost tunnel, Alaska. *Permafrost and Periglacial Processes* **6**: 120-128 DOI:
513 10.1002/ppp.709.
514 Ducharme M-A, Allard M, Côté J, L'Hérault E. 2015. Measurements of permafrost thermal
515 conductivity through CT-scan analysis. In *Proceedings GeoQuébec 2015– 68th Canadian*
516 *Geotechnical Conference & 7th Canadian Permafrost Conference, 20-23 September 2015,*
517 *Quebec, Canada*.

518 Fortier D, Kanevskiy M, Shur Y. 2008. Genesis of reticulate-chaotic cryostructure in
519 permafrost. In *Proceedings of the Ninth International Conference on Permafrost, June 29*
520 *– July 3, 2008, Fairbanks, Alaska*, Kane DL, Hinkel KM (eds). Institute of Northern
521 Engineering, University of Alaska Fairbanks, Vol. 1; 451-456.
522 Fortier D, Kanevskiy M, Shur Y, Stephani E, Dillon M, Jorgenson T. 2012. Cryostructures of
523 basal glacier ice as an object of permafrost study: observations from the Matanuska
524 Glacier, Alaska. In *Proceedings of the Tenth International Conference on Permafrost,*
525 *June 25-29, 2012, Salekhard, Russia*, Hinkel KM (ed). The Northern Publisher: Salekhard,
526 Russia; Vol. 1: International contributions; 107-112.
527 Fotiev SM. 2014. Massive ice beds, Marre-Sale Cape (western coast of the Yamal Peninsula).
528 *Earth Cryosphere* **XVIII** (2), 34-46. (in Russian)
529 Fotiev SM. 2015. Genesis and mechanism of formation of repeated-intrusive massive ice
530 layers. *Earth Cryosphere* **XIX** (1): 27-36.
531 French H, Shur Y. 2010. The principles of cryostratigraphy. *Earth-Science Reviews* **101**: 190-
532 206. DOI: 10.1016/j.earscirev.2010.04.002.
533 Fritz M, Wetterich S, Meyer H, Schirrmeister L, Lantuit H, Pollard WH. 2011. Origin and
534 characteristics of massive ground ice on Herschel Island (western Canadian arctic) as
535 revealed by stable water isotope and hydrochemical signatures. *Permafrost and*
536 *Periglacial Processes* **22** (1): 26–38. DOI: 10.1002/ppp.714.
537 Fritz M, Wetterich S, Shirrmeister L, Meyer H, Lantuit H, Preusser F, Pollard WH. 2012.
538 East Beringia and beyond: Late Wisconsinan and Holocene landscape dynamics along the
539 Yukon Coastal Plain, Canada. *Palaeogeography, Palaeoclimatology, Palaeoecology* **319-**
540 **320**: 28-45. DOI: 10.1016/j.palaeo.2011.12.015.

541 Froese DG, Zazula GD, Westgate JA, Preece SJ, Sanborn PT, Reyes AV, Pearce NJG. 2009.
542 The Klondike goldfields and Pleistocene environments of Beringia. *GSA Today* **19**(8): 4-
543 10. DOI: 10.1130/GSATG54A.1
544 Grosse G, Robinson JE, Bryant R, Taylor MD, Harper W, DeMasi A, Kyker-Snowman E,
545 Veremeeva A, Schirrmeister L, Harden J. 2013. Distribution of late Pleistocene ice-rich
546 syngenetic permafrost of the Yedoma Suite in East and Central Siberia, Russia. USGS
547 Geological Survey Open-File Report 2013-1078, 37 pp.
548 Härtel S, Christiansen HH, Elberling B. 2012. Cryostratigraphy and ice content of the near-
549 surface permafrost in lower Adventdalen, Svalbard. In *Proceedings of the Tenth*
550 *International Conference on Permafrost, June 25-29, 2012, Salekhard, Russia*. The
551 Northern Publisher: Salekhard, Russia; Vol. 4: Extended Abstracts; 207-208.
552 Iwahana G, Fukui K, Mikhailov N, Ostanin O, Fujii Y. 2012. Structure of a Lithalsa in the
553 Akkol Valley, Russian Altai Mountains. *Permafrost and Periglacial Processes* **23** (2):
554 107–118. DOI: 10.1002/ppp.1734.
555 Jorgenson, T., Kanevskiy, M.Z., Shur, Y., Moskalenko, N.G., Brown, D.R.N., Wickland, K.,
556 Striegl, R., and Koch, J. (2015) Ground ice dynamics and ecological feedbacks control
557 ice-wedge degradation and stabilization. JGR Earth Surface 120 (11): 2280-2297.
558 doi:10.1002/2015JF003602.
559 Kanevskiy M, Fortier D, Shur Y, Bray M, Jorgenson T. 2008. Detailed cryostratigraphic
560 mapping of syngenetic permafrost in the Winze of the CRREL Permafrost Tunnel, Fox,
561 Alaska. In *Proceedings of the Ninth International Conference on Permafrost, Fairbanks,*
562 *U.S.A.*; 889-894.
563 Kanevskiy M, Shur Y, Jorgenson MT, Stephani E. 2011. Cryostratigraphy of late Pleistocene
564 syngenetic permafrost (yedoma) in northern Alaska, Itkillik River exposure. *Quaternary*
565 *Research* **75**: 584-596. DOI: 10.1016/j.yqres.2010.12.003.

566 Kanevskiy M, Shur Y, Connor B, Dillon M, Stephani E, O'Donnell J. 2012. Study of the ice-
567 rich syngenetic permafrost for road design (Interior Alaska). In *Proceedings of the Tenth*
568 *International Conference on Permafrost, June 25-29, 2012, Salekhard, Russia,* Hinkel KM
569 (ed). The Northern Publisher: Salekhard, Russia; Vol. 1: International contributions; 191-
570 196.
571 Kanevskiy M, Shur Y, Krzewinski T, Dillon M. 2013a. Structure and properties of ice-rich
572 permafrost near Anchorage, Alaska. *Cold Regions Science and Technology* **93**: 1-11. DOI:
573 10.1016/j.coldregions.2013.05.001.
574 Kanevskiy M, Shur Y, Jorgenson MT, Ping C-L, Michaelson GJ, Fortier D, Stephani E,
575 Dillon M, Tumskoy V. 2013b. Ground ice in the upper permafrost of the Beaufort Sea
576 coast of Alaska. *Cold Regions Science and Technology* **85**: 56-70. DOI:
577 10.1016/j.coldregions.2012.08.002.
578 Kanevskiy M, Jorgenson MT, Shur Y, O'Donnell JA, Harden JW, Zhuang Q, Fortier D.
579 2014. Cryostratigraphy and permafrost evolution in the lacustrine lowlands of West-
580 Central Alaska. *Permafrost and Periglacial Processes* **25**: 14-34. DOI: 10.1002/ppp.1800.
581 Katasonov EM. 2009. Lithology of frozen Quaternary deposits (cryolithology) of the Yana
582 Coastal Plain (PhD thesis, Obruchev Permafrost Institute, 1954). Ed. Kaplina, T.N.
583 Moscow, PNIIIS, 176 pp. (in Russian)
584 Konishchev VN. 2009. Climate warming and permafrost. Moscow State University.
585 *Geography-Environment-Sustainability* **1**: 4-19.
586 Konishchev VN. 2011. Permafrost response to climate warming. *Earth Cryosphere* **XV** (4):
587 13-16.
588 Kritsuk LN. 2010. Ground ice of West Siberia. Moscow, Nauchniy Mir, 352 pp. (in Russian)

589 Kuhry P. 2008. Palsa and peat plateau development in the Hudson Bay Lowlands, Canada:
590 timing, pathways and causes. *Boreas* **37** (2), 316–327. DOI: 10.1111/j.1502-
591 3885.2007.00022.x.
592 Kuhry P, Grosse G, Harden JW, Hughlius G, Koven CD, Ping C-L, Schirrmeister L, Tarnocai
593 C. 2013. Characterization of the permafrost carbon pool. *Permafrost and Periglacial*
594 *Processes* **24**: 146-155. DOI: 10.1002/ppp.1782.
595 Lachniet MS, Lawson DE, Sloat AR. 2012. Revised ^{14}C dating of ice wedge growth in
596 interior Alaska (USA) to MIS 2 reveals cold paleoclimate and carbon recycling in ancient
597 permafrost terrain. *Quaternary Research* **78**: 217-225. DOI: 10.1016/j.yqres.2012.05.007.
598 Lacelle DM, Vasil'chuk YK. 2013. Recent progress (2007-2012) in permafrost isotope
599 geochemistry. *Permafrost and Periglacial Processes* **24** (2): 138-145. DOI:
600 10.1002/ppp.1768.
601 Lacelle D, Fisher DA, Clark ID, Berinstain A. 2008. Distinguishing between vapor- and
602 liquid-formed ground ice in the northern martian regolith and potential for biosignatures
603 preserved in ice bodies. *Icarus* **197**: 458–469. DOI: 10.1016/j.icarus.2008.05.017.
604 Lacelle D, St-Jean M, Lauriol B, Clark ID, Lewkowicz A, Froese DG, Kuehn SC, Zazula.
605 2009. Burial and preservation of a 30,000 year old perennial snowbank in Red Creek
606 valley, Ogilvie Mountains, central Yukon, Canada. *Quaternary Science Reviews* **28**:
607 3401–3413. DOI:10.1016/j.quascirev.2009.09.013
608 Lacelle D, Davila AF, Pollard WH, Andersen D, Heldmann J, Marinova M, McKay CP.
609 2011. Stability of massive ground ice bodies in University Valley, McMurdo Dry Valleys
610 of Antarctica: Using stable O–H isotope as tracers of sublimation in hyper-arid regions.
611 *Earth and Planetary Science Letters* **301**: 403–411. DOI: 10.1016/j.epsl.2010.11.028
612 Lacelle D, Lauriol B, Zazula G, Ghaleb B, Utting N, Clark ID. 2013. Timing of advance and
613 basal conditions of the Laurentide Ice Sheet during the last glacial maximum in the

614 Richardson Mountains, NWT. *Quaternary Research* **80**: 274-283. DOI:
615 10.1016/j.yqres.2013.06.001
616 Lacelle D, Brooker A, Fraser RH, Kokelj SV. 2015. Distribution and growth of thaw slumps
617 in the Richardson Mountains-Peel Plateau region, northwestern Canada. *Geomorphology*
618 **235**: 40-51. DOI: 10.1016/j.geomorph.2015.01.024
619 Lapalme CM, Lacelle D, Davila AF, Pollard W, Fortier D, McKay CP. 2015.
620 Cryostratigraphy of near-surface permafrost in University Valley, McMurdo Dry Valleys
621 of Antarctica. In *Proceedings GeoQuébec 2015– 68th Canadian Geotechnical Conference*
622 *& 7th Canadian Permafrost Conference, 20-23 September 2015, Quebec, Canada*.
623 Lauriol B, Lacelle D, St-Jean M, Clark ID, Zazula GD. 2010. Late Quaternary
624 paleoenvironments and growth of intrusive ice in eastern Beringia (Eagle River valley,
625 northern Yukon, Canada). *Canadian Journal of Earth Sciences* **47**: 941–955. DOI:
626 10.1139/E10-012.
627 Leibman MO, Kizyakov AI, Lein AYu, Perednya DD, Savvichev AS, Vanshtein BG. 2011.
628 Sulfur and carbon isotopes within atmospheric, surface and ground water, snow and ice as
629 indicators of the origin of tabular ground ice in the Russian Arctic. *Permafrost and*
630 *Periglacial Processes* **22** (1): 39-48. DOI: 10.1002/ppp.716.
631 Mackay JR. 1972. The world of underground ice. *Annals of the American Association of*
632 *Geographers* **62**: 1-22. DOI: 10.1111/j.1467-8306.1972.tb00839.x.
633 Mackay JR. 1990. Some observations on the growth and deformation of epigenetic,
634 syngenetic and anti-syngenetic ice wedges. *Permafrost and Periglacial Processes* **1**: 15-
635 29. DOI: 10.1002/ppp.3430010104.
636 Mackay JR, Dallimore SR. 1992. Massive ice in the Tuktoyaktuk area, western Arctic coast,
637 Canada. *Canadian Journal of Earth Sciences* **29** (6): 1235-1249. DOI: 10.1139/e92-099.

638 Mel'nikov VP, Spesivtsev VI. 2000. Cryogenic formations in the earth's lithosphere. Siberian
639 Publishing Center UIGGM, Siberian Branch, Russian Academy of Sciences, Novosibirsk.
640 Meyer H, Yoshikawa K, Schirrmeister L, Andreev A. 2008. The Vault Creek Tunnel
641 (Fairbanks Region, Alaska) – A Late Quaternary Palaeoenvironmental Permafrost Record.
642 In *Proceedings of the Ninth International Conference on Permafrost, June 29 – July 3,*
643 *2008, Fairbanks, Alaska*. Kane DL, Hinkel KM (eds). Institute of Northern Engineering,
644 University of Alaska Fairbanks, Vol. 2, 1191-1196.
645 Meyer H, Schirrmeister L, Andreev A, Wagner D, Hubberten HW, Yoshikawa K, Bobrov A,
646 Wetterich S, Opel T, Kandiano E, Brown J. 2010. Lateglacial and Holocene isotopic and
647 environmental history of northern coastal Alaska – results from a buried ice-wedge system
648 at Barrow. *Quaternary Science Reviews* **29**: 3720-3735. DOI:
649 10.1016/j.quascirev.2010.08.005.
650 Michel FA. 2011. Isotope characterisation of ground ice in northern Canada. *Permafrost and*
651 *Periglacial Processes* **22**: 3–12. DOI: 10.1002/ppp.721.
652 Morse PD, Burn CR. 2013. Field observations of syngenetic ice wedge polygons, outer
653 Mackenzie Delta, western Arctic coast, Canada. *Journal of Geophysical Research: Earth*
654 *Surface* **118**: 1320-1332. DOI: 10.1002/jgrf.20086.
655 Murton JB. 2009. Stratigraphy and palaeoenvironments of Richards Island and the eastern
656 Beaufort Continental Shelf during the last glacial–interglacial cycle. *Permafrost and*
657 *Periglacial Processes* **20**: 107–125. DOI: 10.1002/ppp.647.
658 Murton JB. 2013. Ground ice and cryostratigraphy. In *Treatise on Geomorphology, Vol. 8,*
659 *Glacial and Periglacial Geomorphology,* Schoder JF (editor-in-chief), Giardino R,
660 Harboor J (volume eds). Academic Press: San Diego; 173-201.
661 Murton JB, Goslar T, Edwards ME, Bateman MD, Danilov PP, Savvinov GN, Gubin SV,
662 Ghaleb B, Haile J, Kanevskiy M, Lozhkin AV, Lupachev AV, Murton DK, Shur Y,

Tikhonov A, Vasil'chuk AC, Vasil'chuk YK, Wolfe SA. 2015. Paleoenvironmental interpretation of yedoma silt (ice complex) deposition as cold-climate loess, Duvanny Yar, northeast Siberia. *Permafrost and Periglacial Processes* **26**: 208-288. DOI: 10.1002/ppp.1843.

O'Neill HB, Burn CR. 2012. Physical and temporal factors controlling the development of near-surface ground ice at Illisarvik, western Arctic coast, Canada. *Canadian Journal of Earth Sciences* **49**: 1096-1110. DOI: 10.1139/E2012-043.

Opel T, Dereviagin AYu, Meyer H, Schirrmeister L, Wetterich S. 2011. Palaeoclimatic Information from Stable Water Isotopes of Holocene Ice Wedges on the Dmitrii Laptev Strait, Northeast Siberia, Russia. *Permafrost and Periglacial Processes* **22** (1): 84-100. DOI: 10.1002/ppp.667.

Osterkamp TE, Jorgenson MT, Schuur EAG; Shur YL, Kanevskiy MZ, Vogel JG, Tumskoy VE. 2009. Physical and ecological changes associated with warming permafrost and thermokarst in interior Alaska. *Permafrost and Periglacial Processes* **20**: 235-256. DOI: 10.1002/ppp.656.

Phillips M, Burn C, Wolfe S, Morse P, Gaanderse A, O'Neill B, Shugar D, Gruber S. 2015. Improving water content description of ice-rich permafrost soils. In *Proceedings GeoQuébec 2015– 68th Canadian Geotechnical Conference & 7th Canadian Permafrost Conference, 20-23 September 2015, Quebec, Canada*.

Popov AI. 2013. Selected works, and about him. Moscow, Nauchniy Mir, 536 pp. (in Russian)

Pumple J, Froese D, Calmels F. 2015. Characterizing permafrost valley fills along the Alaska Highway, southwest Yukon. In *Proceedings GeoQuébec 2015– 68th Canadian Geotechnical Conference & 7th Canadian Permafrost Conference, 20-23 September 2015, Quebec, Canada*.

688 Raffi R, Stenni B. 2011. Isotopic composition and thermal regime of ice wedges in northern
689 Victoria Land, East Antarctica. *Permafrost and Periglacial Processes* **22** (1): 65-83. DOI:
690 10.1002/ppp.701.
691 Reyes AV, Froese DG, Jensen BJL. 2010. Permafrost response to last interglacial warming:
692 field evidence from non-glaciated Yukon and Alaska. *Quaternary Science Reviews* **29**:
693 3256–3274. DOI: 10.1016/j.quascirev.2010.07.013.
694 Riddle CH, Rooney JW. 2012. Encounters with relict permafrost in the Anchorage, Alaska,
695 area. In *Proceedings of the Tenth International Conference on Permafrost*, Salekhard,
696 Yamal-Nenets Autonomous District, Russia, June 25-29, 2012 1: 323-328.
697 Rogov VV. 2009. Fundamentals of cryogenesis (textbook). Novosibirsk, Geo, 203 pp. (in
698 Russian)
699 Schirrmeister L, Kunitsky V, Grosse G, Wetterich S, Meyer H, Schwamborn G, Babiy O,
700 Derevyagin A, Siegert C. 2011. Sedimentary characteristics and origin of the Late
701 Pleistocene Ice Complex on north-east Siberian Arctic coastal lowlands and islands – A
702 review. *Quaternary International* **241**: 3-25. DOI: 10.1016/j.quaint.2010.04.004.
703 Schirrmeister L, Froese D, Tumskoy V, Grosse G, Wetterich S. 2013. Yedoma: Late
704 Pleistocene ice-rich syngenetic permafrost of Beringia. In *Encyclopedia of Quaternary*
705 *Science*, Second Edition, Elias SA, Mock CJ (eds). Elsevier: Amsterdam, Vol. **2**: 542-552.
706 Seppälä M. 2011. Synthesis of studies of palsa formation underlining the importance of local
707 environmental and physical characteristics. *Quaternary Research* **75**: 366-370. DOI:
708 10.1016/j.yqres.2010.09.007.
709 Sharkuu N, Yoshikawa K, Anarmaa S. 2012. Perennial frost mounds in Mongolia. In
710 *Proceedings of the Tenth International Conference on Permafrost, June 25-29, 2012,*
711 *Salekhard, Russia*, Hinkel KM (ed). The Northern Publisher: Salekhard, Russia; Vol. 1:
712 International contributions, 371-376.

713 Shpolyanskaya NA. 2015. Pleistocene-Holocene history of permafrost evolution in the
714 Russian Arctic based on ground-ice studies. Moscow-Izhevsk, Institute of Computer
715 Researches, 344 pp. (in Russian)
716 Shur YL. 1988. The upper horizon of permafrost soils. Proceedings of the Fifth International
717 Conference on Permafrost. Tapir Publishers, Trondheim: Norway, Vol. 1, 867-871.
718 Shur YL, Jorgenson MT. 1998. Cryostructure development on the floodplain of the Colville
719 River Delta, northern Alaska. In *Proceedings of the Seventh International Conference on*
720 *Permafrost. Collection Nordicana* **57**: 993-999.
721 Shur YL, Jorgenson MT, Kanevskiy MZ. 2011. Permafrost. In *Encyclopedia of Earth*
722 *Sciences Series, Encyclopedia of Snow, Ice and Glaciers*, Singh VP, Singh P, Haritashya
723 UK (eds). Springer: Netherlands: 841-848. DOI: 10.1007/978-90-481-2642-2.
724 Shur YL, Kanevskiy M, Jorgenson T, Dillon M, Stephani E, Bray M. 2012. Permafrost
725 degradation and thaw settlement under lakes in yedoma environment. In *Proceedings of*
726 *the Tenth International Conference on Permafrost, June 25-29, 2012, Salekhard, Russia,*
727 Hinkel KM (ed). The Northern Publisher: Salekhard, Russia; Vol. 1: International
728 contributions, 383-388.
729 Skurikhin AN, Gangodagamage C, Rowland JC, Wilson CJ. 2013. Arctic tundra ice-wedge
730 landscape characterization by active contours without edges and structural analysis using
731 high-resolution satellite imagery. *Remote Sensing Letters* **4**: 1077-1086. DOI:
732 10.1080/2150704X.2013.840404.
733 Slagoda EA, Leibman MO, Opokina OL. 2010. Origin of deformations in Holocene-
734 Quaternary deposits with tabular ground ice on Yugorsky peninsula. *Earth Cryosphere*
735 **XIV** (4): 30-41. (in Russian)
736 Slagoda EA, Opokina OL, Kurchatova AN, Rogov VV. 2012a. Structure and composition of
737 complex massive ice bodies in Late Pleistocene-Holocene sediments of the Marre-Sale

738 Cape, West Yamal. In *Proceedings of the Tenth International Conference on Permafrost,*
739 *25–29 June 2012, Salekhard, Russia*, Melnikov VP, Drozdov DD, Romanovsky VE (eds):
740 415–420.
741 Slagoda EA, Opokina OL, Rogov VV, Kurchatova AN. 2012b. Structure and genesis of the
742 underground ice in the Neopleistocene-Holocene sediments of Marre-Sale cape, Western
743 Yamal. *Earth Cryosphere* **XVI** (2): 9-22. (in Russian)
744 Sliger M, Fortier D, deGrandpré I, Lapointe-Elmrabti L. 2015. Incidence of pleistocene-
745 holocene climate on the concurrent landscape and permafrost development of the Beaver
746 Creek region, southwest Yukon, Canada. In *Proceedings GeoQuébec 2015– 68th Canadian*
747 *Geotechnical Conference & 7th Canadian Permafrost Conference, 20-23 September 2015,*
748 *Quebec, Canada*.
749 Solomatin VI. 2013. Physics and geography of underground glaciation. Novosibirsk, Geo,
750 346 pp. (in Russian)
751 Solomatin VI, Belova NG. 2012. Proof of the glacier origin of tabular massive ice. In
752 *Proceedings of the Tenth International Conference on Permafrost, June 25-29, 2012,*
753 *Salekhard, Russia*, Melnikov VP, Drozdov DS, Romanovsky VE (eds). The Northern
754 Publisher: Salekhard, Russia; Vol. 2: Translations of Russian contributions, 427-432.
755 Spektor VB, Spektor VV, Bakulina NT. 2008. New data on the Ice Complex of the Lena-
756 Amga rivers plain (Central Yakutia). In *Proceedings of the Ninth International*
757 *Conference on Permafrost, University of Alaska Fairbanks, Fairbanks*, Vol 2: 1681–1684.
758 Spektor VB, Spektor VV, Bakulina NT. 2011. Buried Snow in the Lena-Amga Plain. *Earth*
759 *Cryosphere* **15** (4): 16-21. (in Russian)
760 Stephani E, Kanevskiy M, Dillon M, Bray M, Shur Y. 2012. Cryostratigraphy of Yedoma
761 (Ice Complex) in Seward Peninsula, Alaska. In *Tenth International Conference on*

762 *Permafrost, June 25-29, 2012, Salekhard, Russia*. Vol. 4/2: Extended abstracts. Fort
763 Dialog-Iset: Ekaterinburg, Russia: 569-570.
764 Stephani E, Fortier D, Shur Y, Fortier R, Doré G. 2014. A geosystems approach to
765 permafrost investigations for engineering applications, an example from a road
766 stabilization experiment, Beaver Creek, Yukon, Canada. *Cold Regions Science and*
767 *Technology* **100**: 20-35. DOI: 10.1016/j.coldregions.2013.12.006.
768 St-Jean M, Lauriol B, Clark ID, Lacelle D, Zdanowicz C. 2011. Investigation of ice-wedge
769 infilling processes using stable oxygen and hydrogen isotopes, crystallography and
770 occluded gases (O_2, N_2, Ar). *Permafrost and Periglacial Processes* **22**: 49-64. DOI:
771 10.1002/ppp.680.
772 Strauss J, Schirrmeister L, Wetterich S, Borchers A, Davydov SP. 2012. Grain-size properties
773 and organic-carbon stock of Yedoma Ice Complex permafrost from the Kolyma lowland,
774 northeastern Siberia. *Global Biogeochemical Cycles* **26:** GB3003. DOI:
775 10.1029/2011GB004104.
776 Strauss J, Schirrmeister L, Grosse G, Wetterich S, Ulrich M, Herzschuh U, Hubberten H-W.
777 2013. The deep permafrost carbon pool of the Yedoma region in Siberia and Alaska.
778 *Geophysical Research Letters* **40**(23): 6165-6170. DOI: 10.1002/2013GL058088.
779 Streletskaya ID, Vasilev AA. 2012 The ice complex of western Taymyr. In *Proceedings of*
780 *the Tenth International Conference on Permafrost, June 25-29, 2012, Salekhard, Russia,*
781 Melnikov VP, Drozdov DS, Romanovsky VE (eds). The Northern Publisher: Salekhard,
782 Russia; Vol. 2: Translations of Russian contributions, 433-438.
783 Streletskaya I, Vasiliev A, Meyer H. 2011. Isotopic composition of syngenetic ice wedges
784 and palaeoclimatic reconstruction, western Taymyr, Russian Arctic. *Permafrost and*
785 *Periglacial Processes* **22**: 101-106. DOI: 10.1002/ppp.707.

786 Tumskoy VE. 2012. Peculiarities of cryolithogenesis in Northern Yakutia (middle
787 Neopleistocene to Holocene). *Earth Cryosphere* **XVI** (1): 2-21. (in Russian)
788 Ulrich M, Grosse G, Strauss J, Schirrmeister L. 2014. Quantifying Wedge-Ice Volumes in
789 Yedoma and Thermokarst Basin Deposits. *Permafrost and Periglacial Processes* **25**: 151-
790 161. DOI: 10.1002/ppp.1810.
791 van Everdingen RO. (Ed.). 1998 revised May 2005. Multi-language Glossary of Permafrost
792 and Related Ground-ice Terms. Boulder, CO: National Snow and Ice Data Center/World
793 Data Center for Glaciology.
794 Vasil'chuk AC, Vasil'chuk YK. 2010. Local pollen spectra as a new criterion for nonglacial
795 origin of massive ice. *Transactions (Doclady) of Russian Academy of Sciences, Earth*
796 *Sciences* **433**: 985–990. DOI: 10.1134/S1028334X10070305.
797 Vasil'chuk AC, Vasil'chuk YK. 2012. Pollen and Spores as Massive Ice Origin Indicators. In
798 *Proceedings of the Tenth International Conference on Permafrost, June 25-29, 2012,*
799 *Salekhard, Russia,* Melnikov VP, Drozdov DD, Romanovsky VE (eds). The Northern
800 Publisher: Salekhard, Russia; Vol. 2, 487-492.
801 Vasil'chuk YK. 2009. New approach to estimation of wedge-ice volume. *Inzhenernaya*
802 *Geologiya (Engineering Geology)* **4**: 40-47. (in Russian)
803 Vasil'chuk YK. 2012. Classification of Massive Ice. In *Proceedings of the Tenth*
804 *International Conference on Permafrost, June 25-29, 2012, Salekhard, Russia,* Melnikov
805 VP, Drozdov DD, Romanovsky VE (eds). The Northern Publisher: Salekhard, Russia;
806 Vol. 2, 493–497.
807 Vasil'chuk YK. 2013. Syngenetic ice wedges: cyclical formation, radiocarbon age and stable
808 isotope records by Yurij K. Vasil'chuk, Moscow University Press, Moscow, 2006, 404
809 pp., ISBN 5-211-05212-9. (Monograph Synopsis) *Permafrost and Periglacial Processes*
810 **24**: 82-93. DOI: 10.1002/ppp.1764.

811 Vasil'chuk YK, Vasil'chuk AC, Budantseva NA, Chizhova JN, Papesch W, Podborny YY,
812 Sulerzhitsky LD. 2009. Oxygen Isotope and Deuterium Indication of the Origin and ^{14}C
813 Age of the Massive Ice, Bovanenkovo, Central Yamal Peninsula. *Doklady Earth Sciences*
814 **429**: 1326–1332. DOI: 10.1134/S1028334X09080194.
815 Vasil'chuk YK, Budantseva NA., Vasil'chuk AC. 2011. Variations in $\delta^{18}O$, δD, and the
816 concentration of pollen and spores in autochthonic heterogeneous massive ice on the
817 Erkutayaha River in the southern part of the Yamal Peninsula. *Doklady Earth Sciences*
818 **438**: 721–726. DOI: 10.1134/S1028334X11050382.
819 Vasil'chuk YK, Vasil'chuk AC, Budantseva NA. 2012. Isotopic and palynological
820 compositions of a massive ice in the Mordyyakha River, Central Yamal Peninsula.
821 *Doklady Earth Sciences* **446**: 1105–1109. DOI: 0.1134/S1028334X12090164.
822 Vasil'chuk YK, Budantseva NA, Vasilchuk AC, Yoshikawa K, Podborny YY, Chizhova JN.
823 2014. Isotope composition of pingo ice core in the Evoyakha river valley, North-West
824 Siberia. *Earth Cryosphere* **XVIII** (4): 47-58. (in Russian)
825 Vasil'chuk YK, Alexeev SV, Arzhannikov SG, Alexeeva LP, Budantseva NA, Chizhova JN,
826 Arzhannikova AV, Vasil'chuk AC. 2015 (in press). Lithalsas in the Sentsa River Valley,
827 Eastern Sayan Mountains, Southern Russia. *Permafrost and Periglacial Processes*. DOI:
828 10.1002/ppp.1876
829 Vasiliev AA, Streletskaya ID, Melnikov VP, Oblogov GE. 2015. Methane in ground ice and
830 frozen Quaternary deposits of West Yamal. *Doklady Akademii Nauk [Transactions of*
831 *Academy of Sciences] Earth Sciences* **465** (2): 1289-1292, DOI:
832 10.1134/S1028334X15120168
833 Wetterich S, Rudaya N, Tumskoy V, Andreev AA, Opel T, Schirrmeister L, Meyer H. 2011.
834 Last Glacial Maximum records in permafrost of the East Siberian Arctic. *Quaternary*
835 *Science Reviews* **30**: 3139-3151. DOI: 10.1016/j.quascirev.2011.07.020.

Wetterich S, Tumskoy V, Rudaya N, Andreev AA, Opel T, Meyer H, Schirrmeister L, Hüls M. 2014. Ice Complex formation in arctic East Siberia during the MIS3 Interstadial. *Quaternary Science Reviews* **84**: 39-55. DOI: 10.1016/j.quascirev.2013.11.009.

Wolfe SA, Stevens CW, Gaanderse AJ, Oldenborger G. 2014. Lithalsa distribution, morphology and landscape associations in the Great Slave Lowland, Northwest Territories, Canada. *Geomorphology* **204**: 302-313. DOI: 10.1016/j.geomorph.2013.08.014.

Wünnemann B, Reinhardt C, Kotlia BS, Riedel F. 2008. Observations on the relationship between lake formation, permafrost activity and lithalsa development during the last 2000 years in the Tso Kar Basin, Ladakh, India. *Permafrost and Periglacial Processes* **19**: 341-358. DOI: 10.1002/ppp.631.

Yoshikawa K, Sharkhuu N, Sharkhuu A. 2013. Groundwater hydrology and stable isotope analysis of an open-system pingo in Northwestern Mongolia. *Permafrost and Periglacial Processes* **24**: 175-183. DOI: 10.1002/ppp.1773.

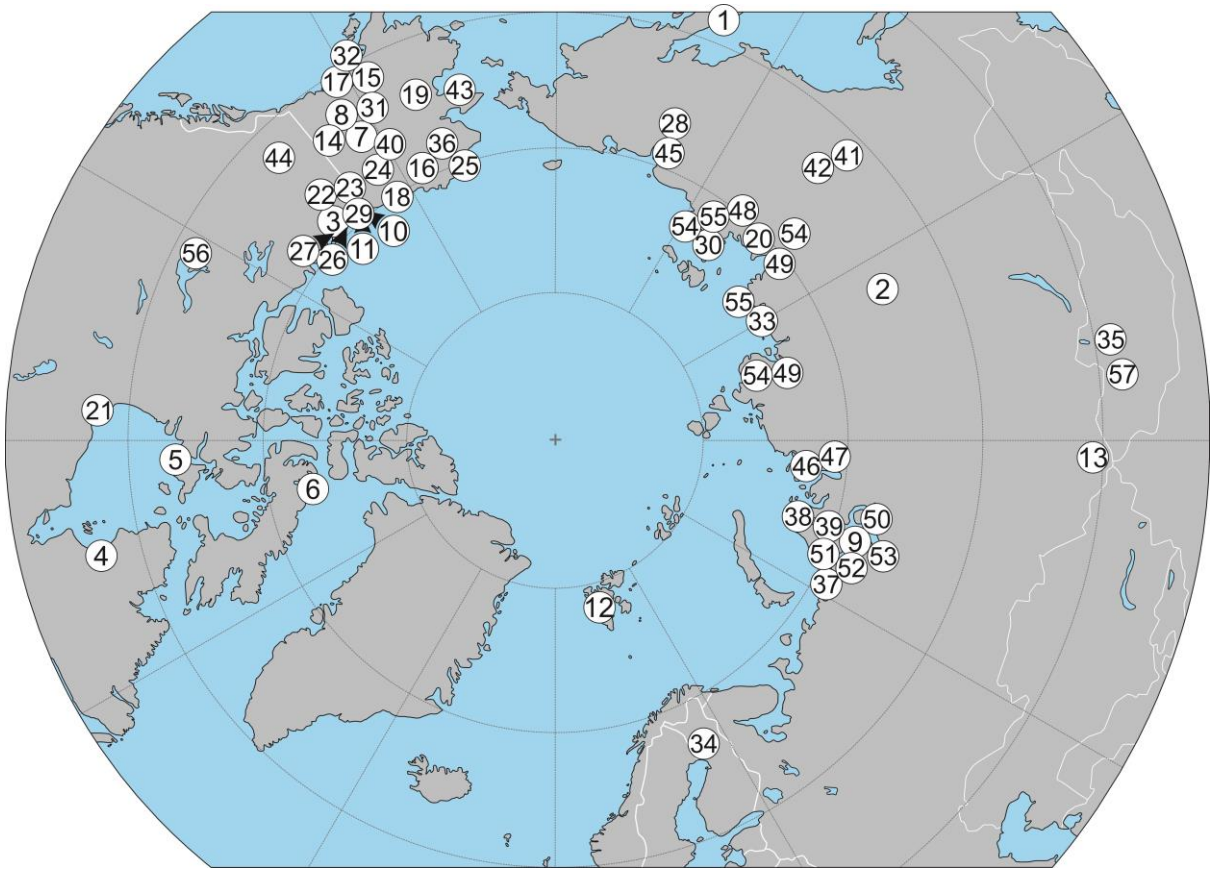

851

852 **Figure 1.** Approximate locations of field investigations included in this review. Regional
853 studies and investigations which predate 2008 are not included. 1) Abramov *et al.*, 2008; 2)
854 Alexeev *et al.*, 2016; 3) Bode *et al.*, 2008; 4) Calmels *et al.*, 2008; 5) Calmels *et al.*, 2012; 6)
855 Coulombe *et al.*, 2015; 7) Douglas *et al.*, 2011; 8) Fortier *et al.*, 2012; 9) Fotiev, 2014; 10)
856 Fritz *et al.*, 2011; 11) Fritz *et al.*, 2012; 12) Härtel *et al.*, 2012; 13) Iwahana *et al.*, 2012; 14)
857 Kanevskiy *et al.*, 2008; 15) Kanevskiy *et al.*, 2011; 16) Kanevskiy *et al.*, 2012; 17)
858 Kanevskiy *et al.*, 2013a; 18) Kanevskiy *et al.*, 2013b; 19) Kanevskiy *et al.*, 2014; 20)
859 Katasonov, 2009; 21) Kuhry, 2008; 22) Lacelle *et al.*, 2009; 23) Lauriol *et al.*, 2010; 24)
860 Meyer *et al.*, 2008; 25) Meyer *et al.*, 2010; 26) Morse and Burn, 2013; 27) Murton, 2009; 28)
861 Murton *et al.*, 2015; 29) O'Neill and Burn, 2012; 30) Opel *et al.*, 2011; 31) Osterkamp *et al.*,
862 2009; 32) Riddle and Rooney, 2012; 33) Schirrmeister *et al.*, 2011; 34) Seppälä, 2011; 35)
863 Sharkuu *et al.*, 2012; 36) Shur *et al.*, 2012; 37) Slagoda *et al.*, 2010; 38) Slagoda *et al.*,
864 2012a; 39) Slagoda *et al.*, 2012b; 40) Sliger *et al.*, 2015; 41) Spektor *et al.*, 2011; 42) Spektor

865 *et al.*, 2008; 43) Stephani *et al.*, 2012; 44) Stephani *et al.*, 2014; 45) Strauss *et al.*, 2012; 46)
866 Streletskaya and Vasilev, 2012; 47) Streletskaya *et al.*, 2011; 48) Tumskoy, 2012; 49) Ulrich
867 *et al.*, 2014; 50) Vasil'chuk *et al.*, 2014; 51) Vasil'chuk *et al.*, 2009; 52) Vasil'chuk *et al.*,
868 2011; 53) Vasil'chuk *et al.*, 2012; 54) Wetterich *et al.*, 2011; 55) Wetterich *et al.*, 2014; 56)
869 Wolfe *et al.*, 2014; 57) Yoshikawa *et al.*, 2013.

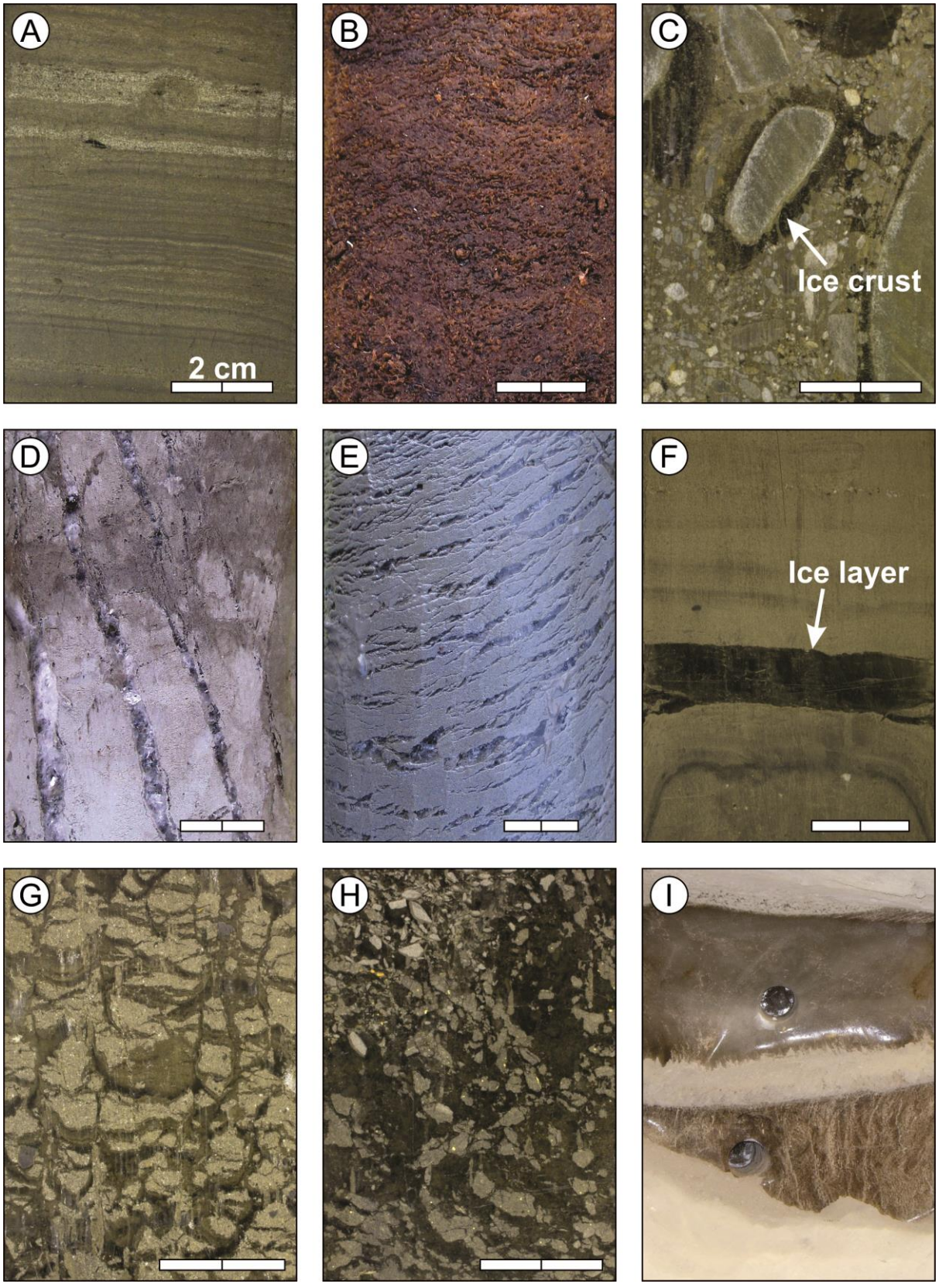

Figure 2. Simplified classification of cryostructures in unconsolidated sediments. All photographs are oriented vertically such that the long-axis of the image is perpendicular to

the ground surface. A) Pore cryostructure, note the absence of visible ice. B) Organic-matrix cryostructure, ice present in the void space but not visible. C) Crustal cryostructure. D) Vein cryostructure. E) Lenticular cryostructure. F) Layered cryostructure. G) Reticulate cryostructure. H) Ataxitic cryostructure. I) Solid cryostructure – thermokarst-cave (pool) ice overlying a vertically foliated ice wedge. Two drill holes several cm in diameter are visible in the ice. Based on a classification presented by Murton (2013), which is modified from previous classifications.

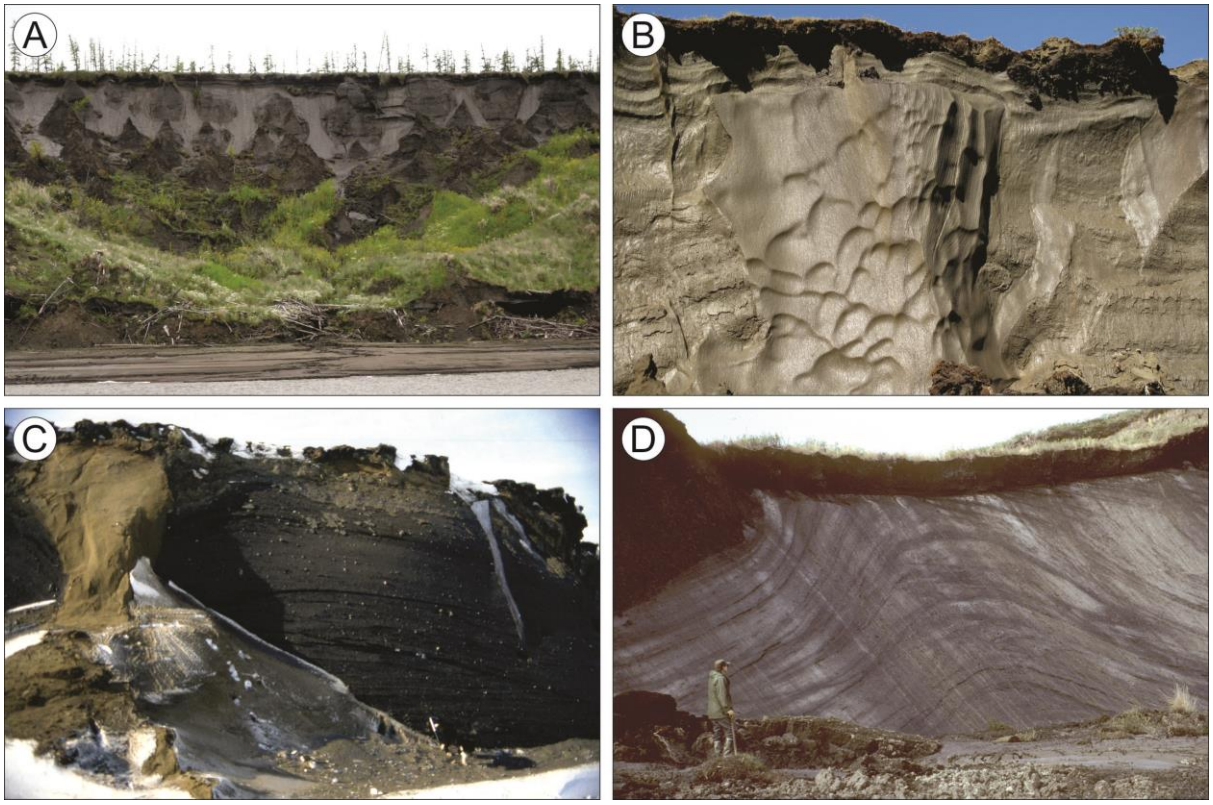

Figure 3. A) Yedoma exposed in headwall of a retrogressive thaw slump at Duvanny Yar, northeast Yakutia, Russia. Syngenetic ice wedges (lighter-coloured grey) enclose columns of silt (darker-coloured grey), some of which degrade to form conical thermokarst mounds (baydzherakhs). Top of headwall is about 39 m above the level of the Kolyma River (in foreground); B) Ice-rich ca. 1-m-thick intermediate layer with thin active ice wedge on top of large buried syngenetic ice wedge, 35-m-high Itkillik River yedoma exposure, northern Alaska; C) Buried basal ice from the Laurentide Ice Sheet, Mason Bay, Richards Island, Northwest Territories, Canada. Pebbles and cobbles protrude from surface of massive ice, and folds occur within it. Sand wedge on left and two ice wedges on right penetrate massive ice. Dog and ice axe for scale in bottom centre; D) Post-glacial intrasedimental massive ice at Peninsula Point, near Tuktoyaktuk, Northwest Territories, Canada. Anticline in banded massive underlies a small slump.